 

Selected Paper

# Syntheses of [60]Fullerene and *N*,*N*-Bis(4-biphenyl)aniline-Tethered Rotaxane: Photoinduced Electron-Transfer Processes via Singlet and Triplet States of [60]Fullerene

**Atula S. D. Sandanayaka, Kei-ichiro Ikeshita,[1] Nobuhiro Watanabe,[2] Yasuyuki Araki, Yoshio Furusho,[1,3] Nobuhiro Kihara,[1] Toshikazu Takata,*[,1,2] and Osamu Ito***

Institute of Multidisciplinary Research for Advanced Materials, Tohoku University, Katahira 2-1-1, Aoba-ku, Sendai 980-8577

[1]Department of Applied Chemistry, Graduate School of Engineering, Osaka Prefecture University, 1-1 Gakuen-cho, Sakai, Osaka 599-8531

[2]Department of Organic and Polymeric Materials, Tokyo Institute of Technology, Ookayama, Meguro-ku, Tokyo 152-8552

[3]Yashima Super-Structured Helix Project, JST, Moriyama-ku, Nagoya 463-0003

Received December 17, 2004; E-mail: ito@tagen.tohoku.ac.jp: ttakata@polymer.titech.ac.jp

A rotaxane containing [60]fullerene ($C_{60}$) and *N*,*N*-bis(4-biphenyl)aniline (BBA) moieties was synthesized. In this structure, $C_{60}$ acting as an electron acceptor, is attached to the crown-ether ring through which the axle with terminal BBA moieties acting as electron donors on both ends is penetrating. This rotaxane had a neutral amide moiety in the center of the axle in which two BBA moieties act as stoppers. The intra-rotaxane photoinduced electron-transfer processes of the $C_{60}$ and BBA moieties were investigated by time-resolved transient absorption and fluorescence measurements while changing solvent polarity and temperature. Time-resolved transient absorption measurements of the rotaxanes confirmed that the long-lived charge-separated state ($C_{60}^{\bullet -}$; $BBA^{\bullet +}$)$_{rotaxane}$ was formed via both the excited singlet and triplet states of $C_{60}$ ($^1C_{60}$* and $^3C_{60}$*, respectively) in polar solvents. The rate constants for charge-separation process were evaluated to be in the range of $(3.6–3.7) \times 10^8$ $s^{-1}$ via $^1C_{60}$* and $(5.1–5.6) \times 10^7$ $s^{-1}$ via $^3C_{60}$* in the ratio of (0.36–0.38):(0.43–0.51). The rate constants of charge recombination were $2.5 \times 10^6$ $s^{-1}$ and $4.4 \times 10^6$ $s^{-1}$, corresponding to the lifetimes of the charge-separated states of 400 ns and 230 ns in THF and benzonitrile, respectively. By the temperature dependences, the activation free-energy changes of charge-separation process via $^3C_{60}$* were evaluated to be 0.10 eV, while those of the charge-recombination process were estimated to be 0.03 eV in THF and benzonitrile. These low activation energies are one of the characteristics of through-space electron transfer in the rotaxanes.

A new, rapidly progressing field on the crossroad between chemistry and supramolecular chemistry has just emerged as an interdisciplinary field of science and technology with interesting perspectives.[1–3] With the advance of supramolecular chemistry, efficient synthetic routes of rotaxanes have been built-up exploiting the ability of assistance from cooperative noncovalent bonding interactions. [60]Fullerene ($C_{60}$) derivatives have shown a wide range of physical and chemical properties that make them attractive for the preparation of supramolecular assemblies and new advanced materials for optoelectronic and molecular electronic devices.[4–8] In addition, the unique geometry of these molecules provides templates with an enormous scope for a variety of studies including investigations of energy- and electron-transfer processes within supramolecular assemblies containing the $C_{60}$ moieties under the photoillumination.[9–12] Covalent linkages of $C_{60}$ with specific electron donors involving the electron-mediating and hole-transfer reagents have been extensively studied revealing fast and efficient charge-separation (CS) via the excited singlet states of the $C_{60}$ derivatives ($^1C_{60}$*) and/or donor molecules, resulting in long lived CS states.[13–15] Supramolecules composed of the coordination bonds between the $C_{60}$–pyridine derivatives and zinc porphyrins have also been studied, showing fast and efficient CS process via the excited singlet states of zinc porphyrins and/or the $C_{60}$ derivatives; in these cases, the CS states with lifetimes longer than ca. 100 ns were not observed yet.[4,16] The high steady-state concentration of the CS state is very important for the successful use of these molecular systems for energy-conversion devices. The strategy has been developed to investigate the rates of electron-transfer (ET) process in these supramolecular systems by tuning the energies of the donor–acceptor pair, and by optimizing the distance and orientation between the donor–acceptor.

Recently, rotaxanes containing the $C_{60}$ moiety as electron acceptors and phthalocyanine and porphyrin as electron donors were synthesized, of which $C_{60}$ moiety was spatially placed with respect to the phthalocyanine and porphyrin moieties. In these rotaxanes, it has been reported that the CS process takes place via the excited singlet states of these chromophores.[17,18]

Published on the web June 6, 2005; DOI 10.1246/bcsj.78.1008

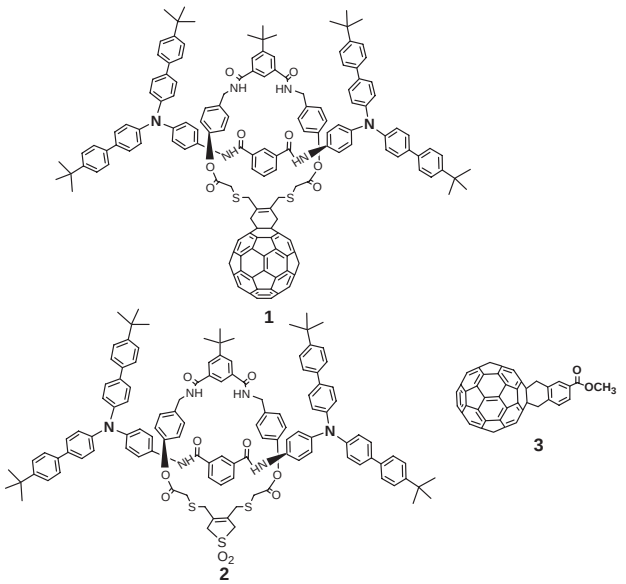


Fig. 1. Molecular structures of rotaxanes **1** and **2** and $C_{60}$-reference **3**.

When the aromatic amines were employed as electron-donors, photoinduced ET processes for $C_{60}$–amine mixture systems have gained a great attention,[19–23] and a vast variety of $C_{60}$–amine dyads, triads, and more complex systems have been synthesized and investigated.[24,25] In most covalently connected dyad systems of $C_{60}$ and aromatic amines such as *N*,*N*-dimethylaniline and triphenylamine (TPA), excitation of the $C_{60}$ moiety initiates electron transfer from the $^1C_{60}$* moiety, generating the CS states ($C_{60}^{\bullet-}$–amine$^{\bullet+}$) with relatively short lifetimes.[25] In our previous paper, however, we reported that the CS process of rotaxanes of fullerene and TPA ($(C_{60};TPA)_{rotaxane}$) predominantly takes place via the excited triplet state of $C_{60}$ ($^3C_{60}$*), and that the CS state ($(C_{60}^{\bullet-};TPA^{\bullet+})_{rotaxane}$) was kept for a relatively long time (170–300 ns) in rotaxane.[26] In the present study, we synthesized a $C_{60}$–[2]rotaxane with *N*,*N*-bis(4-biphenyl)aniline (BBA) moieties as electron donors, as shown in Fig. 1; here, $C_{60}$–BBA [2]rotaxane was abbreviated as **1** or $(C_{60};BBA)_{rotaxane}$. In this rotaxane, we chose the BBA moiety as the amine donor, because it has been reported that the BBA moiety showed quite a long CS state when the BBA moiety was covalently connected with $C_{60}$ ($C_{60}$–BBA dyad);[27] In **1**, BBA moieties are attached to both ends of the axle component, which penetrates the amide-based macrocycle bearing a $C_{60}$ unit. [2]Rotaxane without the $C_{60}$ unit (**2**) and the 4-methoxy-carbonyl-*o*-quinodimethane adduct with $C_{60}$ (**3**) were used as reference compounds.

For the rotaxane **1**, we have investigated the photoinduced ET processes using the time-resolved transient absorption and fluorescence measurements with changing solvent polarity and temperature, expecting longer lifetimes of $(C_{60}^{\bullet-};BBA^{\bullet+})_{rotaxane}$ than those of $(C_{60}^{\bullet-};TPA^{\bullet+})_{rotaxane}$. Furthermore, the CS process of $C_{60}$–BBA dyad efficiently takes place via the $^1C_{60}$* moiety. Thus, it would be anticipated that the contribution of the CS mechanism via the $^1C_{60}$* moiety in $(C_{60};BBA)_{rotaxane}$ may increase. Our aim in this study was to compare these reported photoinduced ET processes in the mixture and covalently connected dyads with newly synthesized rotaxane **1**, in which the through-space electron transfer would be anticipated.

## Experimental

**Syntheses General.** Melting points were measured on a Yanagimoto micro melting point apparatus. IR spectra were recorded on a JASCO FT-IR model 230 spectrometer. $^1$H NMR measurements were performed with JEOL JNM-GX-270 and JNM-L-400 spectrometers in $CDCl_3$ with tetramethylsilane as an internal reference. FAB-MS measurements were performed with a Finnigan TSQ-70 instrument. For preparative HPLC, a JAICO LC-908 system using columns JAIGEL 1 ($\phi$ 20 mm × 600 mm) and JAIGEL 2 ($\phi$ 20 mm × 600 mm) was used. Compounds **7**[28] and **8**[18] were prepared according to the methods described previously. [60]Fullerene was purchased from Frontier Carbon Corporation. Other materials used were the commercially available reagent grade.

**Synthesis of 6:** A mixture of 4-nitroaniline **4** (369 mg, 2.67 mmol), 4-*tert*-butyl-4′-iodobiphenyl **5** (2.37 g, 7.06 mmol), copper powder (684 mg, 10.8 mmol), potassium carbonate (2.97 g, 21.5 mmol), and 18-crown-6 (144 mg, 0.544 mmol) in 1,2-dichlorobenzene (8.0 mL) was refluxed for 2 days under argon atmosphere. The reaction mixture was filtered after being cooled to room temperature. The filtrate was evaporated to dryness. Column chromatographic separation of the mixture on silica gel (chloroform/hexane = 1/1, $R_f = 0.30$) afforded **6** as an orange solid (1.37 g, 2.48 mmol, 93%). mp 97–102 °C (dec.). $^1$H NMR (400 MHz, $CDCl_3$) $\delta$ 8.08–8.05 (m, 2H), 7.60–7.16 (m, 12H), 7.27–7.24 (m, 4H), 7.05–7.02 (m, 2H), 1.37 (s, 18H) ppm. IR (KBr) 3031, 2962, 1587, 1494, 1316 cm$^{-1}$.

**Synthesis of 7:** A suspension of **6** (225 mg, 0.406 mmol) and 5% Pd/C (50.0 mg) in THF (16.0 mL) was stirred at room temperature under $H_2$ atmosphere for 1 day. The catalyst was removed by filtration and the filtrate was evaporated to dryness to yield **7** (213 mg, 0.406 mmol, quant.) as a yellow solid. mp 87–92 °C. $^1$H NMR (270 MHz, $CDCl_3$) $\delta$ 7.63–7.52 (m, 12H), 7.23 (d, $J = 8.6$ Hz, 4H), 7.12 (d, $J = 8.4$ Hz, 2H), 6.72 (d, $J = 8.4$ Hz, 2H), 3.63 (s, 2H), 1.47 (s, 18H) ppm. IR (KBr) 3379, 3030, 2959, 1601, 1495, 1323, 1268 cm$^{-1}$.

**Synthesis of [2]Rotaxane 2:** To a solution of **7** (210 mg, 0.400 mmol) and triethylamine (56.0 μL, 0.401 mmol) in chloroform (20.0 mL) was added a mixture of macrolactam **8**[18] (72.3 mg, 0.100 mmol) and isophthaloyl chloride **9** (20.4 mg, 0.100 mmol) in chloroform (20.0 mL) over a period of 1 h at 0 °C. Then, an additional chloroform solution (10.0 mL) of **9** (20.3 mg, 0.10 mmol) was added over a period of 1 h at 0 °C. After being stirred at 0 °C for 1 h and then at room temperature overnight, the mixture was evaporated to dryness. The residue was purified by column chromatography on silica gel (chloroform, $R_f = 0.05$) and preparative HPLC to afford **2** (43.0 mg, 22.6 μmol, 23% yield based on the macrolactam **8**) as a yellow solid. mp 173–179 °C. $^1$H NMR (400 MHz, $CDCl_3$) $\delta$ 8.89 (s, 1H), 8.33 (s, 2H), 8.27 (s, 2H), 7.99 (s, 1H), 7.87 (d, $J = 7.6$ Hz, 2H), 7.80 (m, 2H), 7.56–7.53 (m, 16H), 7.46 (d, $J = 8.8$ Hz, 8H), 7.44 (m, 1H), 7.40 (d, $J = 8.8$ Hz, 4H), 7.18 (d, $J = 8.8$ Hz, 8H), 7.11 (d, $J = 8.8$ Hz, 4H), 6.84 (d, $J = 8.2$ Hz, 4H), 6.45 (d, $J = 8.2$ Hz, 4H), 4.44 (s, 4H), 3.98 (s, 4H), 3.64 (s, 4H), 3.20 (s, 4H), 1.36 (s, 36H), 1.35 (s, 9H) ppm. IR (KBr) 3365, 2959, 1649, 1601, 1499, 1319, 1272, 1193, 1115, 819 cm$^{-1}$. FAB-MS (matrix: mNBA) *m*/*z* 1901 [M]$^+$.

**Synthesis of [2]Rotaxane 1:** A mixture of $C_{60}$ (61.1 mg, 84.9 μmol), **2** (32.2 mg, 16.9 μmol) and hydroquinone (0.800 mg, 7.26 μmol) in 1,2-dichlorobenzene (15.0 mL) was refluxed for 3 h. The reaction mixture was evaporated to dryness. The residue was chromatographed on silica gel (chloroform, $R_f = 0.10$) and the crude product was purified by preparative HPLC to afford **1** (23.4 mg, 9.14 μmol, 54%) as a blackish brown solid. mp 277–280 °C (dec.). $^1$H NMR (400 MHz, $CDCl_3$, 333 K) $\delta$ 8.97 (s, 1H), 8.44 (s, 2H), 8.37 (s, 2H), 8.16 (s, 1H), 7.99 (d, $J = 7.2$ Hz, 2H), 7.78 (t, $J = 4.0$ Hz, 2H), 7.52–7.48 (m, 21H), 7.40 (d, $J = 8.4$ Hz, 8H), 7.18–7.09 (m, 12H), 6.87 (d, $J = 8.2$ Hz, 4H), 6.52 (d, $J = 8.2$ Hz, 4H), 4.51 (d, $J = 4.0$ Hz, 4H), 4.16 (s, 8H), 3.38 (s, 4H), 1.38 (s, 9H), 1.34 (s, 36H) ppm. IR (KBr) 3422, 2958, 1652, 1496 cm$^{-1}$. FAB-MS (matrix: mNBA) $m/z$ 2560 $[M + H]^+$; Anal. Calcd for $C_{180}H_{120}N_6O_8S_2 \cdot 0.25CHCl_3$: C, 83.62; H, 4.68; N, 3.25; S, 2.48%. Found: C, 83.33; H, 4.68; N, 3.36; S, 2.45%.

**Molecular Orbital Calculation.** An optimized structure and HOMO and LUMO of [2]rotaxane **1** were calculated by the density function B3LYP/3-21G(*) method.[29]

**Electrochemical Measurements.** The cyclic voltammetry measurements were performed on a BAS CV-50W electrochemical analyzer in deaerated benzonitrile solution containing 0.10 M $Bu_4NPF_6$ as a supporting electrolyte at 298 K (100 mV s$^{-1}$). The polished glassy carbon and a platinum wire were used as working electrode and counter electrode, respectively. The measured potentials were recorded with respect to an Ag/AgCl (saturated KCl) reference electrode, using ferrocene/ferrocenium ($Fc/Fc^+$) as an internal reference.

**Spectral Measurements.** Steady-state absorption spectra in the visible and near-IR regions were measured on a Jasco V570 DS spectrometer. Fluorescence spectra were measured on Shimadzu RF-5300PC spectro-fluorophotometer.

Fluorescence lifetimes were measured by a single-photon counting method using a second harmonic generation (SHG, 410 nm) of a Ti:sapphire laser [Spectra-Physics, Tsunami 3950-L2S, 1.5 ps full width at half-maximum (fwhm)] and a streak scope (Hamamatsu Photonics, C4334-01) equipped with a polychromator (Action Research, SpectraPro 150) as an excitation source and a detector, respectively.

Nanosecond transient absorption measurements were carried out using SHG (532 nm) of Nd:YAG laser (Spectra-Physics, Quanta-Ray GCR-130, fwhm 6 ns) as an excitation source. For transient absorption spectra in the near-IR region (600–1600 nm), monitoring light from a pulsed Xe lamp was detected with a Ge-avalanche photodiode (Hamamatsu Photonics, B2834). Details of the transient absorption measurements were described elsewhere.[30,31] All the samples in a quartz cell ($1 \times 1$ cm$^2$) were deaerated by bubbling argon through the solution for 15 min. The temperature dependence of the photoinduced events was measured by immersing the quartz cell in the controlled media in a rectangular quartz Dewar-flask.

## Results and Discussion

**Design, Preparation, and Characterization of [2]Rotaxane 1.** [2]Rotaxane **1** was designed to place spatially the $C_{60}$ and BBA moieties closely each other. They are capable of electron-transferring in the excited state, but do not interact strongly in the ground state. [2]Rotaxane **1** was synthesized by the hydrogen-bonding-assisted method for *sec*-amide-based rotaxanes. Introduction of the fullerene unit was achieved by the Diels–Alder reaction of **2** and $C_{60}$ to afford the fullerene [2]rotaxane **1**. The synthetic route of **1** is outlined in Scheme 1. The Ullman-type coupling of 4-nitroaniline **4** and 4-*tert*-butyl-4′-iodobiphenyl **5** afforded triarylamine **6** in 93% yield. Hydrogenation of **6** catalyzed by 5% Pd/C yielded amine **7**[28] quantitatively. Condensation of **7** with isophthaloyl chloride **9** in the presence of macrolactam **8**[18] gave [2]rotaxane (**2**) bearing a sulfolene moiety on the macrocyclic component in 23% yield. The Diels–Alder reaction of **2** and $C_{60}$ afforded [2]rotaxane (**1**) bearing a $C_{60}$ moiety on the wheel in 54% yield. The structure of **1** was confirmed by $^1$H NMR, IR, FAB-MS, and elemental analysis. As $C_{60}$-reference, 4-methoxycarbonyl-*o*-quinodimethane adduct with $C_{60}$ (**3**) was prepared according to the method described in the literature.[32]

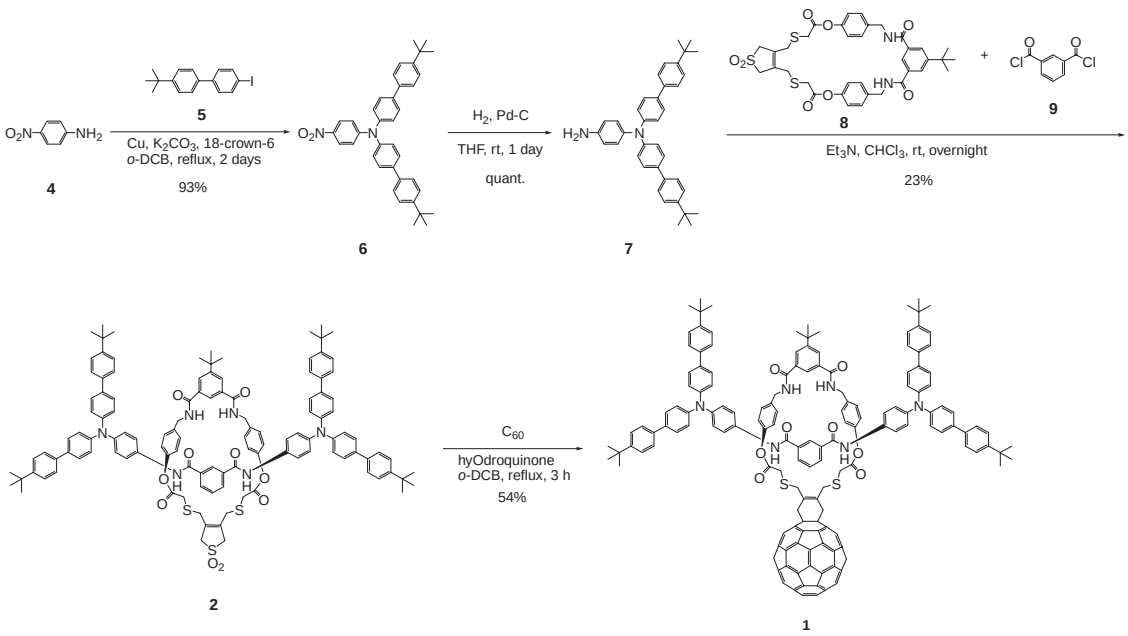


Scheme 1.

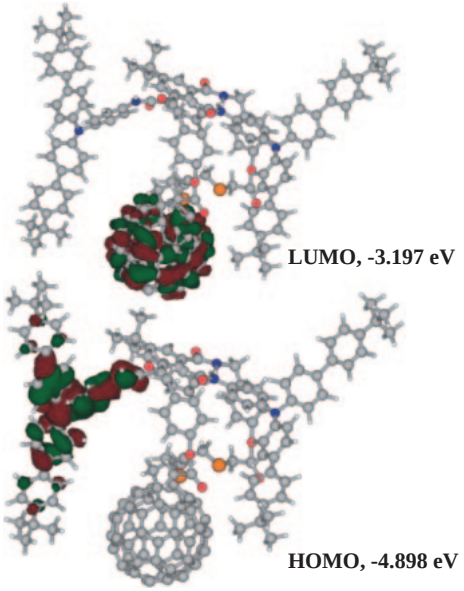


Fig. 2. An optimized structure and HOMO and LUMO of [2]rotaxane **1** calculated by density function B3LYP/3-21G(*) method.

**Optimized Structure and Molecular Orbitals.** An optimized structure and HOMO and LUMO of [2]rotaxane **1** calculated by the density function B3LYP/3-21G(*) method[29] are shown in Fig. 2; the results indicate that rotaxane **1** is not symmetric. One of the two BBA moieties is placed near the $C_{60}$ moiety, while the other BBA moiety is far from the $C_{60}$ moiety. The shorter distance between the center of the $C_{60}$ moiety and the center of the BBA moiety ($R_{CC}$) was estimated to be 10.8 Å, while the longer distance between the center of $C_{60}$ and the center of another BBA was estimated to be 14.1 Å. The center-to-center distance between two BBA moieties is 18.8 Å. The HOMO was located on the BBA moiety near the $C_{60}$ moiety, which corresponds to the radical cation distribution of the CS state, giving the radius of the radical cation ($R_+$) to be 7.1 Å. On the other hand, the LUMO was located on the $C_{60}$ moiety, which corresponds to the radical anion distribution of the CS state, giving the radius of the radical anion ($R_-$) to be 4.7 Å. The HOMO–LUMO gap was evaluated to be 1.7 eV.

**Electrochemical Measurements.** The cyclic voltammograms of [2]rotaxanes **1** and **2** are shown in Fig. 3. The first reduction ($E_{red}$) and oxidation potentials ($E_{ox}$) of rotaxane **1** were estimated to be −1.06 and 0.33 V vs $Fc/Fc^+$ in benzonitrile (PhCN). The former negative potential was attributed to the $E_{red}$ value of the $C_{60}$ moiety and the latter positive potential to the $E_{ox}$ value of the BBA moiety in **1** by comparing with $E_{red}$ of the $C_{60}$ moiety in $C_{60}$-reference **3** (−1.05 V vs $Fc/Fc^+$) and $E_{ox}$ of the BBA moiety in **2** (+0.35 V vs $Fc/Fc^+$) in PhCN. The electrochemical HOMO–LUMO gap was evaluated to be 1.4 eV, which is compatible to the value evaluated from MO calculations. The electrochemical studies revealed that there is no appreciable electronic interaction between the $C_{60}$ and BBA moieties in the ground states.

The free-energy changes of charge-recombination ($\Delta G_{CR}$) of the radical ion-pair states and free-energy changes of

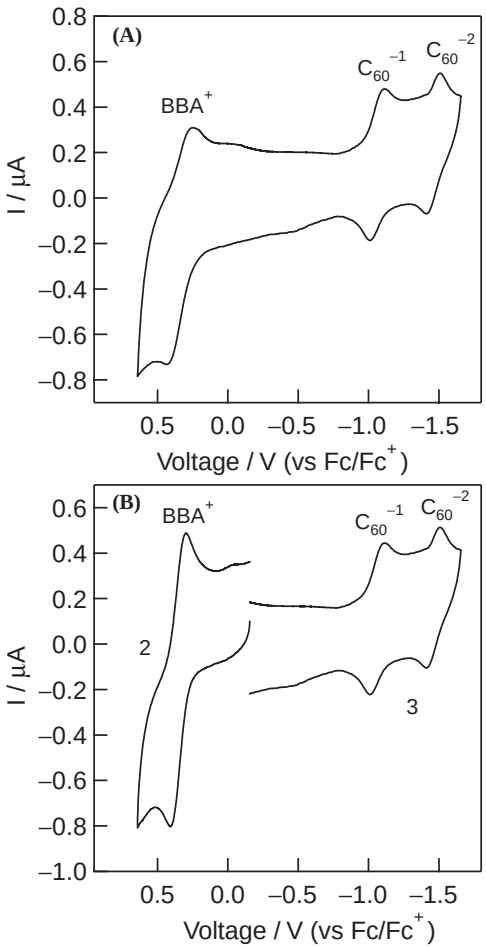


Fig. 3. Cyclic voltammograms of (**A**) [2]rotaxane **1** and (**B**) references **2** and **3** at 100 mV $s^{-1}$ in PhCN.

charge-separation ($\Delta G_{CS}$) were estimated by Eqs. 1 and 2,[33]

$$-\Delta G_{CR} = E_{ox} - E_{red} + \Delta G_s, \quad (1)$$

$$-\Delta G_{CS} = E_0 + \Delta G_{CR}, \quad (2)$$

$$\Delta G_s = e^2/4\pi\varepsilon_0[(1/2R_+ + 1/2R_- - 1/R_{CC})/\varepsilon_s - (1/2R_+ + 1/2R_-)/\varepsilon_R], \quad (3)$$

in which $E_0$ refers the excitation energy of $^1C_{60}$* or $^3C_{60}$*, and $\Delta G_s$ is the correction term which includes the solvent dielectric constants of for photochemistry ($\varepsilon_s$) and electrochemistry ($\varepsilon_R$), respectively, in addition to the vacuum permittivity ($\varepsilon_0$); the radii of the charged donor ($R_+$) and acceptor ($R_-$) evaluated from HOMO and LUMO were employed.

**Steady-State Absorption Measurements.** The steady-state absorption spectra of [2]rotaxanes **1** and **2** and $C_{60}$-reference **3** in toluene are shown in Fig. 4. The absorption peaks at 705 nm and below 350 nm of rotaxane **1** are ascribed to the $C_{60}$ moiety. Since the absorption spectrum **1** is almost a superimposition of reference compounds, **2** and **3**, there is only a weak interaction between the moieties in the ground state of rotaxane **1**. Similar results were obtained for rotaxane **1** in THF and PhCN. Thus, laser photolysis was performed with the 532 nm light, which predominantly excites the $C_{60}$ moiety.

**Steady-State Fluorescence Measurements.** Steady-state fluorescence spectra of [2]rotaxane **1** and $C_{60}$-reference **3** in

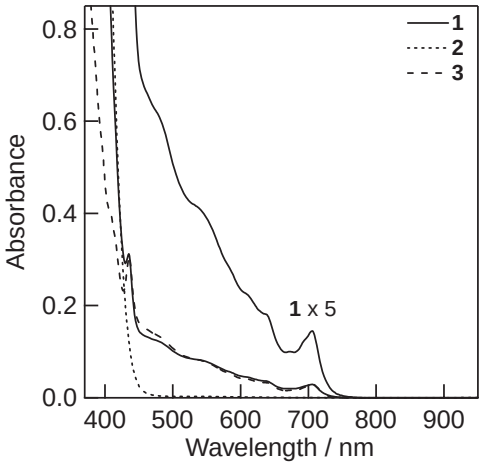


Fig. 4. Steady-state absorption spectra of [2]rotaxane **1** (0.1 mmol dm$^{-3}$), reference **2** (0.1 mmol dm$^{-3}$), and reference **3** (0.1 mmol dm$^{-3}$) in toluene.

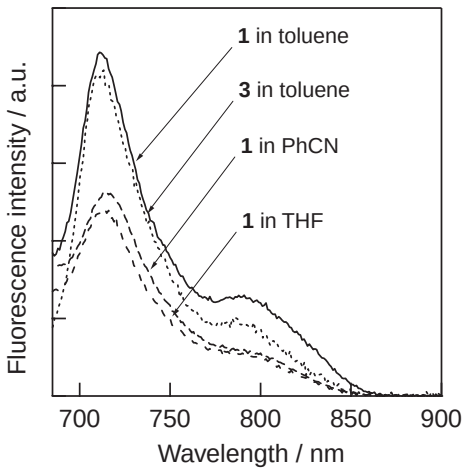


Fig. 5. Steady-state fluorescence spectra of [2]rotaxane **1** and reference **3** (0.1 mmol dm$^{-3}$) in PhCN, THF, and toluene ($\lambda_{ex} = 630$ nm).

toluene, THF, and PhCN ($\lambda_{ex} = 600$ nm) are shown in Fig. 5. The $C_{60}$ moiety of rotaxane **1** and reference **3** shows emission maxima around 715 nm with a shoulder at 780 nm. No evidence for exciplex emission could be obtained, even by decreasing solvent polarity. By comparing the fluorescence peak with the absorption peak (709 nm), rotaxane **1** showed a small Stokes shift. The lowest excited singlet energy of $^1C_{60}$* was evaluated to be 1.75 eV ($E_0(S_1)$).

The fluorescence intensity of **1** at 715 nm in toluene was almost identical to that of **3**. In THF and PhCN, the emission intensities of **1** are smaller than that in toluene by factor of ca. 1/2, while the fluorescence intensity of **1** in toluene is almost the same as those of **3** in PhCN, THF, and toluene. Further quantitative analyses on the fluorescence properties were carried out based on the lifetime measurements.

**Fluorescence Lifetime Measurements.** Figure 6 shows fluorescence decays of of the $^1C_{60}$* moiety in [2]rotaxane **1** in toluene and PhCN obtained by a time-correlated single-photon-counting apparatus with excitation at 410 nm. The fluorescence decay of **1** in toluene was similar to that of **3** in toluene,

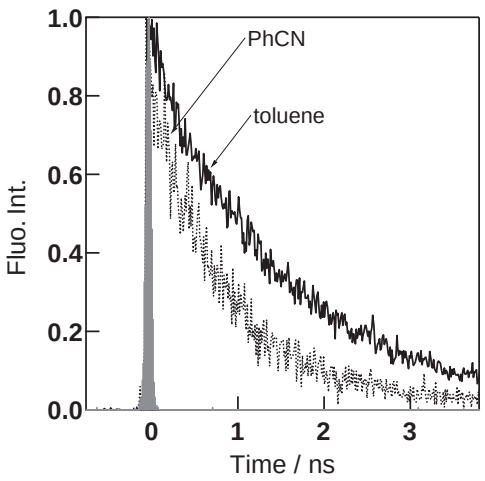


Fig. 6. Fluorescence decay time profiles of [2]rotaxane **1** at 715 nm in PhCN and toluene ($\lambda_{ex} = 410$ nm).

Table 1. Fluorescence Lifetime ($\tau_f$), Rate Constant ($k_{CS}{}^S$),[a] Quantum Yield ($\Phi_{CS}{}^S$),[a] and Free-Energy Changes ($\Delta G_{CS}{}^S$) of CS of [2]Rotaxane **1** in Toluene, THF, and PhCN at Room Temperature

| Solvent | $\tau_f$/ps | $k_{CS}{}^S$/s$^{-1}$ | $\Phi_{CS}{}^S$ | $-\Delta G_{CS}{}^S$/eV |
|---|---|---|---|---|
| Toluene | 1560 | — | — | $-0.05 \pm 0.03$ |
| THF | 980 | $3.8 \times 10^8$ | 0.38 | $0.30 \pm 0.01$ |
| PhCN | 1000 | $3.6 \times 10^8$ | 0.36 | $0.41 \pm 0.01$ |

a) Calculated from Eqs. 4 and 5. b) Calculated from Eqs. 1–3, in which the $E_0$ value of $^1C_{60}$* was set equal to 1.75 eV;[34,35] the errors of $\Delta G_{CS}{}^S$ were estimated when the distances include estimation error of $\pm 0.5$ Å.

which shows almost the same behavior in THF and PhCN. The fluorescence decay of **1** in PhCN, which was almost the same as that in THF, was faster than that in toluene. These fluorescence decays could be fitted as a single-exponential process, giving the fluorescence lifetimes ($\tau_f$) of the $C_{60}$ moiety in rotaxane **1** and reference compound **3** as listed in Table 1. In toluene, the $\tau_f$ value of rotaxane **1** is practically the same as that of **3** (1550–1560 ps), which is referred to as $(\tau_f)_{ref}$. In PhCN and THF, the $\tau_f$ values of rotaxane **1** ($(\tau_f)_{sample}$) are slightly short (980–1000 ps), which is in agreement with the slight quenching of the steady-state fluorescence intensity of $^1C_{60}$* in polar solvents.

From these differences between $(\tau_f)_{sample}$ and $(\tau_f)_{ref}$, the rate constant $k_q{}^S$ and the quantum yield $\Phi_q{}^S$ for fluorescence quenching were evaluated from Eqs. (4) and (5);

$$k_q{}^S = (1/\tau_f)_{sample} - (1/\tau_f)_{ref}, \quad (4)$$

$$\Phi_q{}^S = ((1/\tau_f)_{sample} - (1/\tau_f)_{ref})/(1/\tau_f)_{sample}. \quad (5)$$

The $k_q{}^S$ values are in the range of (3–4) $\times 10^8$ s$^{-1}$ and the $\Phi_q{}^S$ values are in the range of 0.30–0.40 as summarized in Table 1. If one compares these $k_q{}^S$ and $\Phi_q{}^S$ values with the intersystem-crossing (ISC) rate constant ($k_{ISC} = 6.5 \times 10^8$ s$^{-1}$)[30,34] and quantum yields ($\Phi_{ISC} = 0.92$–$0.96$)[30,34] of **3**, one sees that the main process (60–65%) via the $^1C_{60}$* moiety in [2]rotaxane **1** is the ISC process, producing the $^3C_{60}$* moiety even

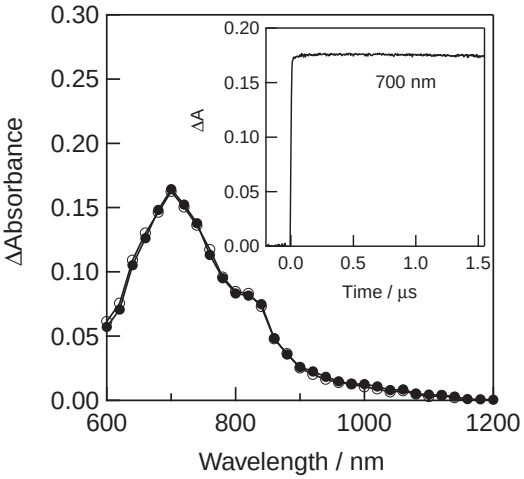


Fig. 7. Nanosecond transient absorption spectra of [2]rotaxane **1** (0.1 mmol dm$^{-3}$) observed by 532 nm laser irradiation in at 0.1 μs (●) and 1.0 μs (○) in toluene. Inset: Absorption-time profiles at 700 nm in toluene.

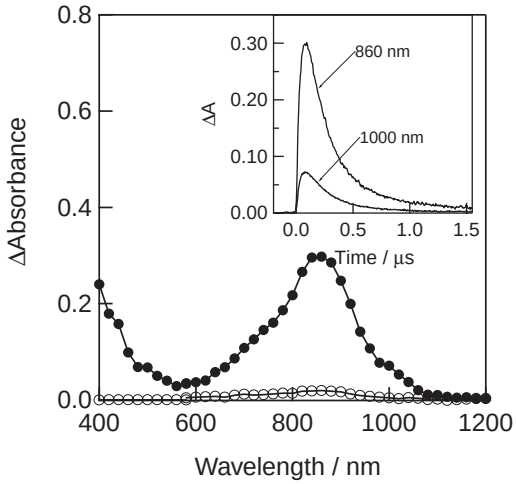


Fig. 8. Nanosecond transient absorption spectra of [2]rotaxane **1** (0.1 mmol dm$^{-3}$) observed by 532 nm laser irradiation in at 0.1 μs (●) and 1.0 μs (○) in PhCN. Inset: Absorption-time profiles at 860 and 1000 nm in PhCN at room temperature.

Table 2. CS Rate Constant ($k_{CS}{}^{T}$), CS Minimum Quantum Yield ($\Phi_{CS}{}^{T}{}_{,min}$) and CS Free Energy ($-\Delta G_{CS}{}^{T}$),[a] and CR Rate Constant ($k_{CR}$) and Lifetime ($\tau_{RIP}$) of Radical Ion-Pair and CR Free Energy ($-\Delta G_{CR}$)[a] of [2]Rotaxane **1** in THF and PhCN

| Solvent | $k_{CS}{}^{T}$ /s$^{-1}$ | $\Phi_{CS}{}^{T}{}_{,min}$ | $\Phi_{CS}{}^{T}{}_{,total}$ | $-\Delta G_{CS}{}^{T}$ /eV | $k_{CR}$ /s$^{-1}$ | $\tau_{RIP}$ /ns | $-\Delta G_{CR}$ /eV |
|---|---|---|---|---|---|---|---|
| THF | $5.1 \times 10^{7}$ | 0.69 | 0.43 | 0.07 | $2.5 \times 10^{6}$ | 400 | 1.45 |
| PhCN | $5.6 \times 10^{7}$ | 0.78 | 0.51 | 0.18 | $4.4 \times 10^{6}$ | 230 | 1.34 |

a) Calculated from Eqs. 1–3; the $E_0$ value of $^3C_{60}$* was set equal to 1.52 eV,[34,35] and estimation error was ±0.01 (see footnote under Table 1).

in the polar solvents.

From the sufficiently negative $\Delta G_{CS}{}^{S}$ values in polar solvents (Table 1), one can conclude that the CS process via the $^1C_{60}$* moiety in rotaxane **1** is a thermodynamically possible process; thus, the $k_q{}^{S}$ and $\Phi_q{}^{S}$ values above can be attributed to the CS process via the $^1C_{60}$* moiety in [2]rotaxane **1**. The CS process can take place in 36–38% of the $^1C_{60}$* moiety, which may be characteristic of [2]rotaxane **1** including the BBA moieties, because this kind of CS process via the $^1C_{60}$* moiety for a similar [2]rotaxane with the TPA moieties is minor (<20%).[26]

**Time-resolved Transient Absorption Spectra.** The time-resolved transient absorption spectrum of [2]rotaxane **1** in toluene observed by nanosecond laser photolysis with 532 nm laser excitation (6 ns laser pulse) is shown in Fig. 7; the spectrum exhibits a peak at 700 nm due to the $^3C_{60}$* moiety in rotaxane **1**, because the same absorption was observed for reference **3** in every solvent under the same experimental conditions. The time profile at 700 nm showed no appreciable decay within a few μs as shown in the inset of Fig. 7.

The transient absorption spectra of [2]rotaxane **1** in PhCN are shown in Fig. 8; in the spectrum observed at 0.1 μs, the main transient absorption band appeared at 860 nm with a shoulder at 1000 nm in addition to the band <500 nm. The absorption bands at 860 nm and <500 nm were attributed to the $BBA^{\bullet+}$ moiety in rotaxane **1**, while the 1000 nm shoulder was assigned to the $C_{60}{}^{\bullet-}$ moiety. By comparing the ratio of the extinction coefficient (40000 mol$^{-1}$ dm$^3$ cm$^{-1}$)[27] at 860 nm of the $BBA^{\bullet+}$ moiety to that of 8500 mol$^{-1}$ dm$^3$ cm$^{-1}$ at 1000 nm of the $C_{60}{}^{\bullet-}$ moiety,[34,35] we could attribute the transient spectrum in PhCN exclusively to the CS state, $(C_{60}{}^{\bullet-};BBA^{\bullet+})_{rotaxane}$. Similarly, the transient absorption spectrum, revealing the formation of $(C_{60}{}^{\bullet-};BBA^{\bullet+})_{rotaxane}$, was obtained in THF for [2]rotaxane **1**.

After reaching the maximum at ca. 0.1 μs, $(C_{60}{}^{\bullet-};BBA^{\bullet+})_{rotaxane}$ began to decay during 100–1200 ns as shown in the inset of Fig. 8. The decays obey first-order kinetics with rate constants in the range of (2.5–4.4) × 10$^6$ s$^{-1}$ in polar solvents, which can be assigned to the CR rate constant ($k_{CR}$), as summarized in Table 2. From the inverse of the $k_{CR}$ values, the lifetimes ($\tau_{RIP}$) of the radical ion-pairs $(C_{60}{}^{\bullet-};BBA^{\bullet+})_{rotaxane}$ are evaluated. The longest $\tau_{RIP}$ value is 400 ns for rotaxane **1** in THF, which is longer than the $\tau_{RIP}$ value (230 ns) for rotaxane **1** in PhCN, suggesting that the CR process belongs in the inverted region of the Marcus parabola.[36]

In the time profile at 1000 nm on the time scale shorter than 100 ns, a rise of the $C_{60}{}^{\bullet-}$ absorption was observed (Fig. 8.). From the curve fitting with a single exponential, the CS rates ($k_{CS}{}^{T}$) via the $^3C_{60}$* moiety were evaluated as listed in Table 2 for rotaxane **1** in polar solvents. The $k_{CS}{}^{T}$ values are in the range of (5.1–5.6) × 10$^7$ s$^{-1}$. The $k_{CS}{}^{T}$ value in PhCN is similar to that in THF, which suggests that solvent polarity does not exert much effect.

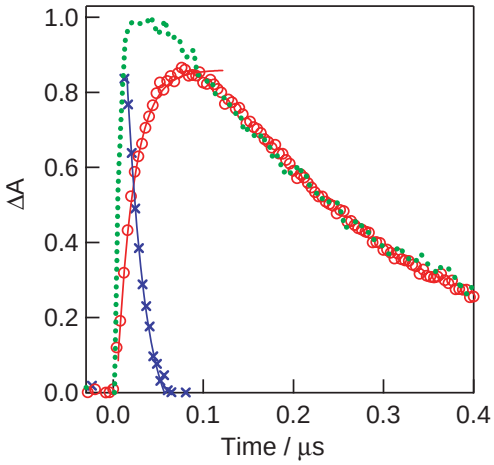


Fig. 9. Absorption-time profiles of [2]rotaxane **1** at 700 nm (green, ···), 1000 nm (red, ○), and subtracted profile from 700 nm (blue, ×) in PhCN.

From the inspection of the time profiles of $(C_{60}^{\bullet-};BBA^{\bullet+})_{rotaxane}$ at 860 and 1000 nm (Fig. 8) at early times (10–100 ns), one can observe a slow rise after the laser pulse of ca. 6 ns. One can assume that the radical ion-pair $(C_{60}^{\bullet-};BBA^{\bullet+})_{rotaxane}$ is obtained via the $^3C_{60}$* moiety as well as the $^1C_{60}$* moiety. Figure 9 shows the time profile at 700 nm in PhCN, in which the rapid decay of the absorption of the $^3C_{60}$* moiety and the rise of the $BBA^{\bullet+}$ moiety in rotaxane **1** may be overlapped. If one assumes that the rise curve for the $BBA^{\bullet+}$ moiety was the same as that of the $C_{60}^{\bullet-}$ moiety at 1000 nm, the observed 700 nm time profile can be curve-resolved as shown in Fig. 9. The extracted decay rate of the $^3C_{60}$* moiety ($4.8 \times 10^7$ $s^{-1}$) was almost the same as the rise rate of the $C_{60}^{\bullet-}$ moiety at 1000 nm ($5.6 \times 10^7$ $s^{-1}$), confirming that the $C_{60}^{\bullet-}$ moiety and $BBA^{\bullet+}$ moiety are generated via the $^3C_{60}$* moiety.

The quantum yields ($\Phi_{CS}{}^T$) of formations of the CS state in rotaxane **1** via the $^3C_{60}$* moiety were estimated from the ratio of the maximal absorbance at 1000 nm of the $C_{60}^{\bullet-}$ moiety to the initial absorbance at 700 nm of the $^3C_{60}$* moiety by substituting each molar extinction coefficient;[34,35] one can assume that the initial absorbance at 700 nm is predominantly due to the $^3C_{60}$* moiety as shown in Fig. 9. If the initial absorbance at 700 nm of the $^3C_{60}$* may contain the absorption of $BBA^{\bullet+}$ moieties, the $\Phi_{CS}{}^T$ values calculated by this method should be minimum values of $\Phi_{CS}{}^T$, which are refered to as $\Phi_{CS}{}^T{}_{,min}$. Such $\Phi_{CS}{}^T{}_{,min}$ values are in the range of 0.60–0.70, respectively, as summarized in Table 2. Compared with $\Phi_{CS}{}^S$ less than 0.4, the overall CS process quantum yield via the $^3C_{60}$* moiety on the basis of the $^1C_{60}$* moiety ($\Phi_{CS}{}^T{}_{,total}$) can be calculated to be $(1 - \Phi_{CS}{}^S)$ $\Phi_{CS}{}^T{}_{,min}$, which are in the range of 0.43–0.51. Thus, the CS process via $^3C_{60}$* in [2]rotaxane **1**, resulting in formation of $(C_{60}^{\bullet-};BBA^{\bullet+})_{rotaxane}$, is more effective than that via $^1C_{60}$*.

**Temperature Effect.** The charge-separation via $^3C_{60}$* and charge-recombination rate constants of rotaxane **1** showed slight temperature dependences. In PhCN and THF, the $k_{CS}{}^T$ and $k_{CR}$ values decreased with decreasing temperature in each solvent. For example, the $k_{CR}$ values decrease from $3.2 \times 10^6$ $s^{-1}$ at 30 °C to $2.5 \times 10^6$ $s^{-1}$ at −50 °C in THF; this difference

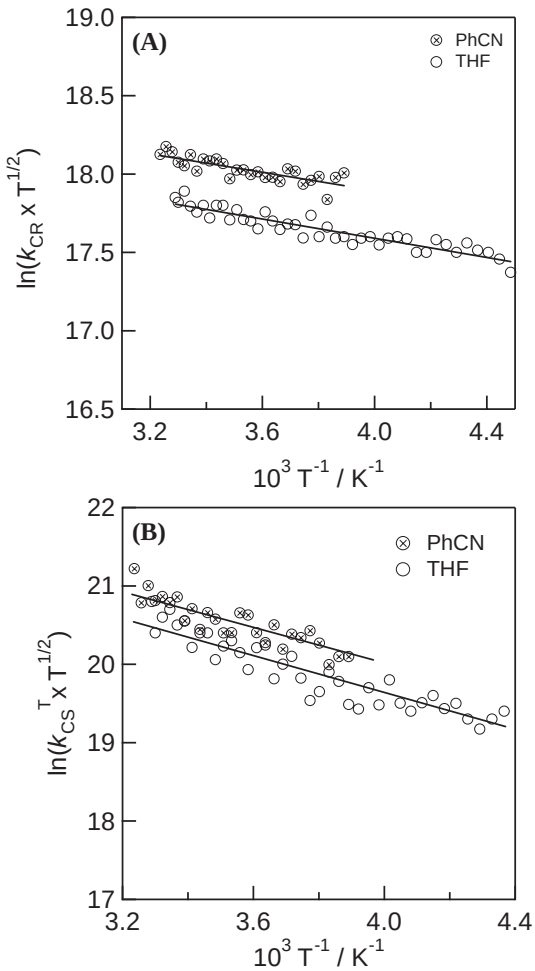


Fig. 10. Modified Arrhenius plots of temperature-dependent (**A**) $k_{CR}$ and (**B**) $k_{CS}$ for [2]rotaxane **1** in PhCN and THF.

is slightly larger than the experimental errors included in our experiments. From a semi-classical Marcus equation, the ET rate constant $k_{ET}$ can be described as follow (Eq. 6):[36]

$$\ln(k_{ET}T^{1/2}) = \ln\{2\pi^{3/2}|V|^2/[h(\lambda k_B)^{1/2}]\} - \Delta G^{\ddagger}/(k_BT). \quad (6)$$

Here $T$, $h$, $k_B$, $|V|$, $\lambda$, and $\Delta G^{\ddagger}$ represent absolute temperature, Planck constant, Boltzmann constant, electron coupling matrix element, reorganization energy, and Gibbs activation energy in the Marcus theory. The plots of $\ln(k_{CS}{}^T \times T^{1/2})$ and $\ln(k_{CR}{}^T \times T^{1/2})$ vs $1/T$ are shown in Fig. 10. Since the slopes are not steep for rotaxane **1**, the $\Delta G^{\ddagger}{}_{CS}{}^T$ and $\Delta G^{\ddagger}{}_{CR}$ values of 0.10–0.11 and 0.03 eV were evaluated, as summarized in Table 3. The $\Delta G^{\ddagger}{}_{CR}$ values in rotaxanes **1** are smaller than those for conventional dyad systems such as the retinyl–$C_{60}$ (0.16 eV).[37] The $\Delta G^{\ddagger}{}_{CS}{}^T$ values less than 0.03 V imply that the CS process occurs without any appreciable energy barrier.[36]

One reason for the quite small $\Delta G^{\ddagger}$ values may be that both processes are dominated mainly by "through-space" electron-transfer process between the $C_{60}$ and BBA chromophores; thus, there is little contribution from any "through-bond" electron-transfer process.[37–39]

Table 3. Activation Free Energy Changes for CS via $^3C_{60}$* ($\Delta G^{\ddagger}_{CS}{}^{T}$) and CR ($\Delta G^{\ddagger}_{CR}$) for [2]Rotaxane **1** in PhCN and THF

| Solvent | $\Delta G^{\ddagger}_{CS}{}^{T}$/eV | $\Delta G^{\ddagger}_{CR}$/eV |
|---|---|---|
| THF | 0.11 | 0.03 |
| PhCN | 0.10 | 0.03 |

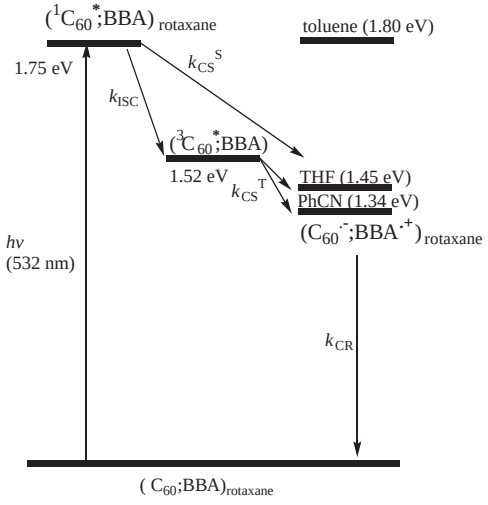


Fig. 11. Schematic energy diagram of [2]rotaxane **1**.

**Energy Diagrams.** From the $\Delta G_{CR}$ and $\Delta G^{S}_{CS}$ values in Tables 1 and 2 in addition to the energy levels of the lowest excited singlet state, the energy diagram for [2]rotaxane **1** can be schematically illustrated as shown in Fig. 11. The $E_0$ values of $^1C_{60}$* and $^3C_{60}$* are reported to be 1.75 and 1.52 eV, respectively.[31,34,35] The energy levels of $(C_{60}{}^{\bullet-};BBA^{\bullet+})_{rotaxane}$ depend on the solvent polarity. Therefore, in toluene since the CS state of rotaxane **1** is slightly higher than the energy level of $^1C_{60}$*, no CS process was observed; thus, $^3C_{60}$* is generated via the ISC process as shown in Fig. 7.[34] In THF and PhCN, the CS states of rotaxane **1** are lower than the energy levels of $^1C_{60}$* and $^3C_{60}$*; thus, the CS process takes place both from the $^1C_{60}$* and $^3C_{60}$* moieties, producing $(C_{60}{}^{\bullet-};BBA^{\bullet+})_{rotaxane}$ in the ratio of (0.36–0.38):(0.43–0.51). The CR process is highly exothermic belonging to the inverted region of the Marcus parabola.[36]

**Comparison with $C_{60}$–BBA Mixture System.** When $C_{60}$ was photoexcited in the presence of excess BBA in PhCN, it was reported in our previous paper that intermolecular electron transfer takes place via $^3C_{60}$* with the rate constant of $6.5 \times 10^8$ mol$^{-1}$ dm$^3$ s$^{-1}$, which is one order smaller than the diffusion-controlled limit.[27] Thus, when the equimolar BBA to $C_{60}$ (0.1 mmol dm$^{-3}$) is present in PhCN, $k_{decay}{}^{first\text{-}order}$ of $^3C_{60}$* and $k_{rise}{}^{first\text{-}order}$ of $C_{60}{}^{\bullet-}$ and $BBA^{\bullet+}$ can be calculated to be $6.5 \times 10^8 \times 10^{-4}$ s$^{-1}$ $= 6.5 \times 10^4$ s$^{-1}$, which is almost the same as $k_{decay}{}^{first\text{-}order}$ of $^3C_{60}$* in the absence of BBA. This indicates that neither appreciable acceleration of the decay of $^3C_{60}$* nor the appearance of $C_{60}{}^{\bullet-}$ and $BBA^{\bullet+}$ was observed in the mixture system. In [2]rotaxane **1** in PhCN, on the other hand, $k_{rise}{}^{first\text{-}order}$ of $C_{60}{}^{\bullet-}$ and $BBA^{\bullet+}$ was obtained to be $5.6 \times 10^7$ s$^{-1}$, which is ca. 1000 times larger than the mixture system. This supports the efficient CS process between the $^3C_{60}$* and BBA moieties spatially placed near each other within [2]rotaxane.

**Comparison with $C_{60}$–BBA Dyads.** For covalently bonded $C_{60}$–BBA, the CS process via the $^1C_{60}$* moiety exclusively takes place in polar solvents, since the $k_{CS}{}^{S}$ and $\Phi_{CS}{}^{S}$ values were evaluated to be $(3.8–5.0) \times 10^{10}$ s$^{-1}$ and 0.98 in THF and PhCN,[27] which are larger than the corresponding values for [2]rotaxane **1**, probably because of the large $|V|$ values for covalently bonded dyads.[38,39] For the CR process of covalently bonded $C_{60}$–BBA, the major rapid and minor slow processes were observed;[27] the rapid CR process can be also due to large $|V|$ values. Although the reliable Marcus parameters of [2]rotaxane **1** were not evaluated in the present study,[40] it is reasonable to consider that the slower ET processes of rotaxane **1** may be ascribed to smaller $|V|$ values compared with those of the covalently connected dyads.

**Comparison with Other Rotaxanes.** Compared with $(C_{60}$:TTP$)_{rotaxane}$, in which the CS process predominantly takes place via $^3C_{60}$* (ca. 70%) compared with via $^1C_{60}$* (<20%),[26] the CS process of $(C_{60}$:BBA$)_{rotaxane}$ via $^1C_{60}$* increases up to 36–38% with decrease in the CS process via $^3C_{60}$* to 43–51%. This may be caused by higher donor ability of the BBA moiety to $^1C_{60}$* ($k_{CS}{}^{S} = (3.6–3.8) \times 10^8$ s$^{-1}$) than that of TPA ($k_{CS}{}^{S} = (1–2) \times 10^8$ s$^{-1}$), probably because the area of BBA is larger than that of TPA in [2]rotaxanes. The $k_{CS}{}^{T}$ values in THF and PhCN of $(C_{60}$:BBA$)_{rotaxane}$ are slightly smaller than those of $(C_{60}$:TPA$)_{rotaxane}$, probably because fluctuation of the distance between the $C_{60}$ and TPA moieties is larger than that between the $C_{60}$ and BBA moieties.[26] The $\tau_{RIP}$ value of $(C_{60}{}^{\bullet-};BBA^{\bullet+})_{rotaxane}$ in THF is longer than those of $(C_{60}{}^{\bullet-};TPA^{\bullet+})_{rotaxane}$, which may be related to the larger size of BBA, in which the radical cation was delocalized.

Compared with rotaxanes with $C_{60}$ and porphyrin moieties[18] and phthalocyanine moieties,[17] in which the CS process takes place mainly via the excited states of the porphyrin and phthalocyanine, we see that the CS process of $(C_{60}$:amine$)_{rotaxane}$ takes place via the excited state of the $C_{60}$ moiety. For the CS process of rotaxanes composed of the $C_{60}$ and zinc porphyrin moiety, contribution of the CS process via the excited triplet state of zinc porphyrin moiety tends to increase with the length of axle, because of increase in the fluctuation.[18b] In the case of rotaxanes composed of Zn porphyrin as an electron donor and Au porphyrins as an electron acceptor, a superexchange mechanism was confirmed.[41] However, for rotaxane **1**, no clear evidence showing the superexchange mechanism was obtained, because of the rather smaller $\pi$-system of BBA moiety.

## Conclusion

For [2]rotaxane **1**, the photoinduced CS process takes place both via the $^3C_{60}$* moiety and via the $^1C_{60}$* moiety, producing long-lived CS state $(C_{60}{}^{\bullet-};BBA^{\bullet+})_{rotaxane}$ in polar solvents. This is one of characteristics of the CS process of rotaxanes, in which through-space electron transfer takes place, although the contribution changes with the electron-donor abilities and the fluctuation ability of the $C_{60}$ and donors moieties in rotaxanes.

This lifetime of $(C_{60}^{\bullet-};BBA^{\bullet+})_{rotaxane}$ was longer than that of the covalently bonded $C_{60}$–BBA dyad system in THF. For the [2]rotaxane **1**, through-space CS and CR processes were also presumed from the low activation free-energies, as evaluated experimentally by the temperature dependence of the CS and CR rate constants.

The present work was supported by Grants-in-Aid for Scientific Research on Priority Areas (417) from the Ministry of Education, Culture, Sports, Science and Technology of Japan.

## References

1 a) J.-M. Lehn, "Supramolecular Chemistry-Concepts and Perspectives," Wiley-VCH, Weinheim (1995). b) F. Vögtle, "Supramolecular Chemistry," Wiley, New York (1991).

2 K. M. Kadish and R. S. Ruoff, "Fullerenes," John Wiley & Sons, New York (2000), p. 225.

3 a) J.-M. Lehn, *Angew. Chem., Int. Ed. Engl.*, **29**, 1304 (1990). b) S. Hannessian, *J. Am. Chem. Soc.*, **117**, 7630 (1995). c) K. R. Seddon and B. A. Christer, *Chem. Soc. Rev.*, **22**, 397 (1993).

4 D. M. Guldi and N. Martín, "Fullerene; From Synthesis and Optoelectronic Propertie," Kluver Academic Publisher, Netherland (2002).

5 D. Gust, T. A. Moore, and A. L. Moore, *Acc. Chem. Res.*, **26**, 198 (1993).

6 N. S. Sacriftci, L. Smilowitz, A. J. Heeger, and F. Wudl, *Science*, **258**, 1474 (1992).

7 a) T. Da Ros, M. Prato, D. M. Guldi, M. Ruzzi, and L. Pasimeni, *Chem.—Eur. J.*, **7**, 816 (2001). b) D. M. Guldi, C. Luo, T. Da Ros, M. Prato, E. Dietel, and A. Hirsch, *Chem. Commun.*, **2000**, 375. c) D. M. Guldi, C. Luo, A. Swartz, M. Scheloske, and A. Hirsch, *Chem. Commun.*, **2001**, 1066. d) F. Diederich and G. M. Lopez, *Chem. Soc. Rev.*, **28**, 263 (1999). e) P. Piotrowiak, *Chem. Soc. Rev.*, **28**, 143 (1999). f) G. Yin, D. Xu, and Z. Xu, *Chem. Phys. Lett.*, **365**, 232 (2002). g) J. R. Weinkauf, S. W. Cooper, A. Schweiger, and C. C. Wamser, *J. Phys. Chem. A*, **107**, 3486 (2003). h) D. M. Guldi, H. Imahori, K. Tamaki, Y. Kashiwagi, H. Yamada, Y. Sakata, and S. Fukuzumi, *J. Phys. Chem. A*, **108**, 541 (2004).

8 a) F. D'Souza, G. D. Deviprasad, M. E. El-Khouly, M. Fujitsuka, and O. Ito, *J. Am. Chem. Soc.*, **123**, 5277 (2001). b) F. D'Souza, G. R. Deviprasad, M. E. Zandler, V. T. Hoang, K. Arkady, M. Van Stipdonk, A. Perera, M. E. El-Khouly, M. Fujitsuka, and O. Ito, *J. Phys. Chem. A*, **106**, 3243 (2002). c) F. D'Souza, G. R. Deviprasad, M. E. Zandler, M. E. El-Khouly, M. Fujitsuka, and O. Ito, *J. Phys. Chem. B*, **106**, 4952 (2002).

9 R. Ballardini, V. Balzani, M. Clemente-León, A. Credi, M. T. Gandolfi, E. Ishow, J. Perkins, J. F. Stoddart, H. R. Tseng, and S. Wenger, *J. Am. Chem. Soc.*, **124**, 12786 (2002).

10 P. Bernier and A. Hirsch, *Carbon*, **38**, 1529 (2000).

11 a) K. Hutchinson, J. Gao, G. Schick, Y. Rubin, and F. Wudl, *J. Am. Chem. Soc.*, **121**, 5611 (1999). b) J. M. Tour, *Acc. Chem. Res.*, **33**, 791 (2000). c) R. M. Metzger, *Acc. Chem. Res.*, **32**, 950 (1999). d) M. A. Fox, *Acc. Chem. Res.*, **32**, 201 (1999).

12 D. Gust, T. A. Moore, and A. L. Moore, *Res. Chem. Intermed.*, **23**, 621 (1997).

13 a) H. Imahori, K. Yamada, M. Hasegawa, S. Taniguchi, T. Okada, and Y. Sakata, *Angew. Chem., Int. Ed. Engl.*, **36**, 2626 (1997). b) H. Imahori, K. Tamaki, D. M. Guldi, C. Luo, M. Fujitsuka, O. Ito, Y. Sakata, and S. Fukuzumi, *J. Am. Chem. Soc.*, **123**, 2607 (2001). c) H. Imahori, Y. Mori, and J. Matano, *J. Photochem. Photobiol., C*, **4**, 51 (2003). d) T. D. M. Bell, T. A. Smith, K. P. Ghiggino, M. G. Ranasinghe, M. J. Shephard, and M. N. Paddon-Row, *Chem. Phys. Lett.*, **268**, 223 (1997).

14 T. Da Ros, M. Prato, D. M. Guldi, E. Alessio, M. Ruzzi, and L. Pasimeni, *Chem. Commun.*, **1999**, 635.

15 F. Diederich and M. G. Lopez, *Chem. Soc. Rev.*, **28**, 263 (1999).

16 P. Piotrowiak, *Chem. Soc. Rev.*, **28**, 143 (1999).

17 a) D. M. Guldi, J. Ramey, M. V. Martinez-Diaz, A. de la Escosura, T. Torres, T. Da Ros, and M. Prato, *Chem. Commun.*, **2002**, 2774. b) K. Li, D. I. Schuster, D. M. Guldi, M. A. Herranz, and L. Echegoyen, *J. Am. Chem. Soc.*, **126**, 3388 (2004).

18 a) N. Watanabe, N. Kihara, Y. Furusho, T. Takata, Y. Araki, and O. Ito, *Angew. Chem., Int. Ed. Engl.*, **42**, 681 (2003). b) A. S. D. Sandanayaka, N. Watanabe, K. Ikeshita, Y. Araki, N. Kihara, Y. Furusho, O. Ito, and T. Takata, *J. Phys. Chem. B*, **109**, 2516 (2005).

19 a) J. W. Arbogast, C. S. Foote, and M. Kao, *J. Am. Chem. Soc.*, **114**, 2277 (1992). b) L. Biczok and H. Linschitz, *Chem. Phys. Lett.*, **195**, 339 (1992). c) S. Nonell, J. W. Arbogast, and C. S. Foote, *J. Phys. Chem.*, **96**, 4169 (1992). d) C. A. Steren, H. von Willigen, L. Biczok, N. Gupta, and H. Linschitz, *J. Phys. Chem.*, **100**, 8920 (1996).

20 a) O. Ito, Y. Sasaki, Y. Yoshikawa, and A. Watanabe, *J. Phys. Chem.*, **99**, 9838 (1995). b) O. Ito, *Res. Chem. Intermed.*, **23**, 389 (1997). c) Y. Yahata, Y. Sasaki, M. Fujitsuka, and O. Ito, *J. Photosci.*, **6**, 11 (1999).

21 H. N. Ghosh, D. K. Palit, A. V. Sapre, and J. P. Mittal, *Chem. Phys. Lett.*, **265**, 365 (1997).

22 J. Senior, A. Z. Szarka, G. R. Smith, and R. M. Hochstrasser, *Chem. Phys. Lett.*, **185**, 179 (1991).

23 G. E. Lawson, A. Kitaygorodskiy, and S. Ya-Ping, *J. Org. Chem.*, **64**, 5913 (1999).

24 a) R. M. Williams, J. M. Zwier, and J. W. Verhoeven, *J. Am. Chem. Soc.*, **117**, 4093 (1995). b) R. M. Williams, M. Koeberg, J. M. Lawson, Y.-Z. An, Y. Rubin, M. N. Paddon-Row, and J. W. Verhoeven, *J. Org. Chem.*, **61**, 5055 (1996).

25 H. Luo, M. Fujitsuka, Y. Araki, O. Ito, P. Padmawar, and L. Y. Chiang, *J. Phys. Chem. B*, **107**, 9312 (2003).

26 A. S. D. Sandanayaka, H. Sasabe, Y. Araki, Y. Furusho, O. Ito, and T. Takata, *J. Phys. Chem. A*, **108**, 5145 (2004).

27 S. Komamine, M. Fujitsuka, O. Ito, K. Moriwaki, T. Miyata, and T. Ohno, *J. Phys. Chem. A*, **104**, 11497 (2000).

28 a) Y. Shirota, K. Moriwaki, S. Yoshikawa, T. Ujike, and H. Nakano, *J. Mater. Chem.*, **8**, 2579 (1998). b) S. Gauthier and J. M. J. Frechet, *Synthesis*, **1987**, 383.

29 M. J. Frich, G. W. Truck, H. B. Schlegel, G. E. Scuseria, M. A. Robb, J. R. Cheeseman, V. G. Zakrzewski, J. A. Montgomery, Jr., R. E. Stratmann, J. C. Burant, S. Dapprich, J. M. Millam, A. D. Daniels, K. N. Kudin, M. C. Strain, O. Farkas, J. Tomasi, V. Barone, M. Cossi, R. Cammi, B. Mennucci, C. Pomelli, C. Adamo, S. Clifford, J. Ochterski, G. A. Petersson, P. Y. Ayala, Q. Cui, K. Morokuma, D. K. Malick, A. D. Rabuck, K. Raghavachari, J. B. Foresman, J. Cioslowski, J. V. Ortiz, A. G. Baboul, B. B. Stefanov, G. Liu, A. Liashenko, P. Piskorz, I. Komaromi, R. Gomperts, R. L. Martin, D. J. Fox, T. Keith, M. A. Al-Laham, C. Y. Peng, A. Nanayakkara, C. Gonzalez, M. Challacombe, P. M. W. Gill, B. Johnson, W. Chen, M. W. Wong, J. L. Andres, C. Gonzalez, M. Head-Gordon, E. S. Replogle, and

J. A. Pople, "Gaussian 98, Revision A.7," Gaussian, Inc., Pittsburgh, PA (1998).

30 A. Watanabe, O. Ito, M. Watanabe, H. Saito, and M. Koishi, *Chem. Commun.*, **1996**, 117.

31 M. M. Alam, A. Watanabe, and O. Ito, *Bull. Chem. Soc. Jpn.*, **70**, 1833 (1997).

32 P. Belik, A. Gugel, A. Kraus, M. Walter, and K. Müllen, *J. Org. Chem.*, **60**, 3307 (1995).

33 A. Z. Weller, *Phys. Chem. Neue Folge*, **133**, 93 (1982).

34 a) R. J. Senion, C. M. Phillips, A. Z. Szarka, W. J. Romanow, A. R. McGhie, Jr., J. P. McCauly, A. P. Smith, and R. M. Hochstrasser, *J. Phys. Chem.*, **95**, 6075 (1991). b) T. W. Ebbesen, K. Tanigaki, and S. Kuroshima, *Chem. Phys. Lett.*, **181**, 501 (1991). c) M. Lee, O.-K. Song, J.-C. Seo, D. Kim, Y. D. Suh, S. M. Jin, and S. K. Kim, *Chem. Phys. Lett.*, **196**, 325 (1992).

35 C. Luo, M. Fujitsuka, A. Watanabe, O. Ito, L. Gan, Y. Huang, and C.-H. Huang, *J. Chem. Soc., Faraday Trans.*, **94**, 527 (1998).

36 a) R. A. Marcus, *J. Chem. Phys.*, **24**, 966 (1956). b) R. A. Marcus, *J. Chem. Phys.*, **43**, 679 (1965). c) R. A. Marcus and N. Sutin, *Biochim. Biophys. Acta*, **811**, 265 (1985).

37 M. Yamazaki, Y. Araki, M. Fujitsuka, and O. Ito, *J. Phys. Chem. A*, **105**, 8615 (2001).

38 a) C. Luo, D. M. Guldi, H. Imahori, K. Tamaki, and Y. Sakata, *J. Am. Chem. Soc.*, **122**, 6535 (2000). b) S. Fukuzumi, H. Imahori, H. Yamada, M. E. El-Khouly, M. Fujitsuka, O. Ito, and D. M. Guldi, *J. Am. Chem. Soc.*, **123**, 2571 (2001). c) H. Imahori, D. M. Guldi, K. Tamaki, Y. Yoshida, Y. C. Luo, Y. Sakata, and S. Fukuzumi, *J. Am. Chem. Soc.*, **123**, 6617 (2001). d) H. Imahori, K. Tamaki, Y. Araki, Y. Sekiguchi, O. Ito, Y. Sakata, and S. Fukuzumi, *J. Am. Chem. Soc.*, **124**, 5165 (2002).

39 a) P. A. Lindell, D. Kuciauskas, J. P. Sumida, B. Nash, D. Nguyen, A. L. Moore, T. A. Moore, and D. Gust, *J. Am. Chem. Soc.*, **119**, 1400 (1997). b) D. Carbonera, M. D. Valentin, C. Corvaja, G. Agostini, G. Giacometti, P. A. Liddell, D. Kuciauskas, A. L. Moore, T. A. Moore, and D. Gust, *J. Am. Chem. Soc.*, **120**, 4398 (1998).

40 We evaluated electron coupling matrix elements in addition to the reorganization energies; although the coupling matrix elements are in the region of 0.1 $cm^{-1}$, the reorganization energies are also extremely small (ca. 0.1 eV). The strict application of semi-classical Marcus equation (Eq. 6) can not be performed such an electron transfer in the inverted region. Thus, we discussed only on the basis of the activation energies in the present study.

41 A. Andersson, M. Linke, J.-C. Chambron, J. Davidsson, V. Heitz, J.-P. Sauvage, and L. Hammarström, *J. Am. Chem. Soc.*, **122**, 3526 (2000).